NeuroImage 134 (2016) 540–549

Contents lists available at ScienceDirect

NeuroImage

journal homepage: www.elsevier.com/locate/ynimg

Dissociated neural substrates underlying impulsive choice and impulsive action

Qiang Wang [a,b], Chunhui Chen [a,b], Ying Cai [a,b], Siyao Li [a,b], Xiao Zhao [a,b], Li Zheng [a,b], Hanqi Zhang [a,b], Jing Liu [a,b], Chuansheng Chen [c], Gui Xue [a,b,*]

[a] State Key Laboratory of Cognitive Neuroscience and Learning & IDG/McGovern Institute of Brain Research, Beijing Normal University, Beijing 100875, PR China
[b] Center for Collaboration and Innovation in Brain and Learning Sciences, Beijing Normal University, Beijing 100875, PR China
[c] Department of Psychology and Social Behavior, University of California, Irvine 92697, United States

ARTICLE INFO

Article history:
Received 17 November 2015
Revised 23 March 2016
Accepted 4 April 2016
Available online 12 April 2016

Keywords:
Impulsive choice
Impulsive action
Delay discounting
Stop-signal task
MVPA
VBM
Resting-state functional connectivity

ABSTRACT

There is a growing consensus that impulsivity is a multifaceted construct that comprises several components such as impulsive choice and impulsive action. Although impulsive choice and impulsive action have been shown to be the common characteristics of some impulsivity-related psychiatric disorders, surprisingly few studies have directly compared their neural correlates and addressed the question whether they involve common or distinct neural correlates. We addressed this important empirical gap using an individual differences approach that could characterize the functional relevance of neural networks in behaviors. A large sample (n = 227) of college students was tested with the delay discounting and stop-signal tasks, and their performances were correlated with the neuroanatomical (gray matter volume, GMV) and functional (resting-state functional connectivity, RSFC) measures, using multivariate pattern analysis (MVPA) and 10-fold cross-validation. Behavioral results showed no significant correlation between impulsive choice measured by discounting rate (k) and impulsive action measured by stop signal reaction time (SSRT). The GMVs in the right frontal pole (FP) and left middle frontal gyrus (MFG) were predictive of k, but not SSRT. In contrast, the GMVs in the right inferior frontal gyrus (IFG), supplementary motor area (SMA), and anterior cingulate cortex (ACC) could predict individuals' SSRT, but not k. RSFC analysis using the FP and right IFG as seed regions revealed two distinct networks that correspond well to the "waiting" and "stopping" systems, respectively. Furthermore, the RSFC between the FP and ventromedial prefrontal cortex (VMPFC) was predictive of k, whereas the RSFC between the IFG and pre-SMA was predictive of SSRT. These results demonstrate clearly neural dissociations between impulsive choice and impulsive action, provide new insights into the nature of impulsivity, and have implications for impulsivity-related disorders.

1. Introduction

The term impulsivity refers to "a tendency to engage in behavior that involves rashness, a lack of foresight or planning, or as a behavior that occurs without reflection or careful deliberation" (Dawe et al., 2004). There is a growing consensus that impulsivity is a multidimensional construct that comprises several components such as impulsive choice and impulsive action (Bari and Robbins, 2013; Dalley et al., 2011; Evenden, 1999). Specifically, impulsive choice is a tendency to prefer small immediate or likely rewards to large delayed or unlikely ones, often measured by the delay discounting task (Ainslie, 1975) as well as other tasks (e.g., Economides et al., 2015; Hare and Neumann, 2008; Robbins, 2002). In contrast, impulsive action reflects a failure of motor inhibition, often measured by the stop-signal task (Logan and Cowan, 1984) or the Go/NoGo task (Donders, 1969). An important question thus concerns whether impulsive choice and impulsive action involve common or distinct neural correlates.

Accumulating evidence has suggested that impulsive choice and impulsive action are the common characteristics of psychiatric disorders such as drug abuse (Bednarski et al., 2012; Fillmore and Rush, 2002; Hu et al., 2015; Kirby et al., 1999; Li et al., 2009; Li et al., 2010; Luo et al., 2013), pathological gambling (Alessi and Petry, 2003), tobacco addiction (Bickel et al., 1999; Billieux et al., 2010), and ADHD (Barkley, 1997; Paloyelis et al., 2010). For example, drug abusers not only prefer immediate but smaller rewards, but also have difficulties in inhibiting prepotent responses (Fillmore and Rush, 2002; Kirby et al., 1999) and show altered inhibitory control processes including response inhibition (Li et al., 2010), error processing (Luo et al., 2013), and conflict anticipation (Hu et al., 2015) during the stop signal task. However, due to the poor understanding of the etiology of these disorders, it is not clear whether these findings reflect a common mechanism of impulsive action and impulsive choice, or the comorbidity of these symptoms.

At the behavioral level, although studies using various questionnaires and scales suggested that the sub-dimensional scores of

* Corresponding author at: State Key Laboratory of Cognitive Neuroscience and Learning, Beijing Normal University, PR China.
E-mail address: guixue@gmail.com (G. Xue).

http://dx.doi.org/10.1016/j.neuroimage.2016.04.010
1053-8119/

impulsive choice (e.g. non-planning impulsiveness and inattention scores) were correlated with impulsive action (e.g. errors of commission and omission) (Lansbergen et al., 2007; Shen et al., 2014; Wilbertz et al., 2014), behavioral tests of impulsive choice (with the delay discounting task) and impulsive action (with stop-signal task) found no strong correlation between them in either rats or humans (Broos et al., 2012; Solanto et al., 2001; van den Bos et al., 2014). In addition, whereas some studies indicated that individuals with higher trait impulsivity measured by Eysenck Personality Questionnaire (EPQ) showed prolonged SSRT (Logan et al., 1997), other studies reported that trait impulsivity measured by Barratt Impulsivity Scale (BIS) was not significantly correlated with SSRT (Farr et al., 2012).

At the neural level, imaging studies often emphasize distinctive frontal–basal ganglia networks for impulsive choice and impulsive action (Aron et al., 2004; Aron et al., 2014; Ghahremani et al., 2012; Peper et al., 2013; Peters and Büechel, 2011). For impulsive choice, it has been suggested that the anterior dorsomedial prefrontal cortex (i.e., frontal pole, FP) is involved in representing temporally more distant reward (Koritzky et al., 2013; Wang et al., 2014). In contrast, the decision value that guides decision is represented in the ventromedial prefrontal cortex and the ventral striatum (Hare et al., 2008; Kable and Glimcher, 2009; Lim et al., 2011), and is modulated by self-control mechanisms implemented in the lateral prefrontal cortex (Hare et al., 2009; Luo et al., 2009; Magen et al., 2014; McClure et al., 2004). In addition, a medial temporo-hippocampal network has also been implicated in perspective evaluation of future outcomes (Bari and Robbins, 2013; Peters and Büechel, 2011).

For impulsive action, existing studies have implicated distributed cortical and subcortical areas for response inhibition, including the right inferior frontal gyrus (IFG) and adjacent anterior insula (AI), anterior cingulate cortex (ACC), pre-SMA, and striatum (Aron et al., 2007b; Aron and Poldrack, 2005; Aron et al., 2004; Aron et al., 2014; Chambers et al., 2009; Chao et al., 2009; Duann et al., 2009; Hampshire and Sharp, 2015; Li et al., 2009; Li et al., 2006; Li et al., 2008; Sharp et al., 2010; Verbruggen and Logan, 2008; White et al., 2014; Zhang and Li, 2012). In particular, whereas the AI–ACC network is important for detecting behaviorally salient events, the right IFG and pre-SMA are important for implementing inhibition (Cai et al., 2014) through the frontostriatal connections (Alexander et al., 1986; Aron and Poldrack, 2006; Seger, 2008).

Using the individual difference approach, several previous studies have further explored the functional relevance of these networks in impulsive choice and impulsive action. For instance, impulsive choice has been linked to the activation level of the ventral striatum (VS) (Beck et al., 2009; Hariri et al., 2006), the GMV of the dorsolateral prefrontal cortex (Bjork et al., 2009), the white matter volume of right prefrontal subgyral region and hippocampus/parahippocampus (Yu, 2012), as well as the structural and functional connectivity between lateral prefrontal cortex and ventral striatum (Peper et al., 2013; van den Bos et al., 2014; van den Bos et al., 2015). In contrast, impulsive action has been linked to the GMVs (Tabibnia et al., 2011; van Gaal et al., 2011) and the fractional anisotropy (FA) of the pre-SMA and IFG (Madsen et al., 2010), the functional and structural connectivity between the IFG and pre-SMA (Aron et al., 2007a; Duann et al., 2009; Neubert et al., 2010), and the preSMA-subthalamic tract strength (Coxon et al., 2012; Forstmann et al., 2012).

To summarize, although many studies have examined the cognitive mechanisms of impulsive choice and impulsive action separately, few have directly compared them. The present study addressed this important empirical gap with an individual difference approach that can explore the functional relevance of different brain regions in impulsive behaviors. A relatively large sample of college students (n = 227) was tested using the delay discounting task and the stop-signal task, which, compared to self-reported assessments, showed improved stability, flexibility, and repeatability (Swann et al., 2002). Their behavioral performance was then correlated with GMV and resting-state functional connectivity (RSFC) data, using a multivariable support vector regression analysis with ten-fold cross-validation (He et al., 2013). Our large sample and the use of cross-validation helped to avoid the unrealistically large correlations obtained from a small sample size with simple correlational analysis (Vul et al., 2009). Based on existing results, we predicted that distinct frontal–subcortical systems would be associated with different aspects of individuals' impulsivity. In particular, the medial prefrontal cortex and ventral striatum would be associated with impulsive choice, whereas the lateral prefrontal cortex, pre-SMA, and dorsal striatum would be associated with impulsive action.

2. Materials and methods

2.1. Participants

Two-hundred and twenty-seven (84 males, 143 females) healthy Chinese college students (18–24 years old, mean age = 20.9 years, SD = 1.17) were recruited for this study. All of them had normal or corrected-to-normal vision and reported no history of psychiatric or neurological disease. Twenty-two additional participants were recruited but excluded from analysis because of short response time (<80 ms) on the stop-signal task (n = 7) or large head motion during fMRI scan (>2 mm) (n = 15). Written informed consent was obtained from each participant after a full explanation of the study purpose and procedure. This study was approved by the Institutional Review Boards of Beijing Normal University and Southwest University.

2.2. Behavioral tasks

The adaptive delay discounting task (van den Bos et al., 2014) and the stop-signal task (Xue et al., 2008) were used to measure individual differences in impulsive choice and impulsive action, respectively. In the adaptive delay discounting task, subjects were presented with a choice between a fixed immediate reward (SS) (RMB 60, approximately USD 10, paid today) and a varied delayed reward (LL) (RMB 78–108, approximately USD 13 to 18, to be paid in 15 to 45 days) (Fig. 1A). We assumed a hyperbolic function ($SV = A / (1 + k * D)$) for temporal discounting, where SV is the subjective value, A the reward magnitude, D the delay time, and k the delay discounting rate. The initial discounting rate was set to 0.02 and was increased when the participants chose the SS option, but decreased when they chose the LL option. For the first 20 trials (out of the total 60 trials), the step size for change of k was set to 0.01 and after that the step size decreased by 5% for each following step. Following previous studies (Johnson and Bickel, 2002; Lagorio and Madden, 2005), hypothetical money was used to serve as a valid proxy for real money.

The stop-signal paradigm consisted of a number of Go trials (75% trials) and Stop trials (25% trials). For each trial, an arrow pointing left or right was displayed on the computer screen. For the Go trials, participants were asked to respond as accurately and quickly as possible with a left or right key press (using the left or right index finger) in 1000 ms. For the Stop trials, a stop signal (red circle) appeared with a stop-signal delay (SSD) subsequent to the arrow stimulus, and participants were asked to withhold the response they already initiated (Fig. 1B). The SSD was determined by a tracking procedure to ensure approximately 50% inhibition rate. Specifically, the SSD would increase by 50 ms when the participants successfully inhibited their response and would decrease by 50 ms when they failed. To reduce participants' anticipation, four step-up and step-down algorithms (staircases) starting with SSD values of 140, 180, 220, and 260 ms were employed. These staircases were interleaved randomly and varied independently (Xue et al., 2008). Each participant finished 4 blocks of 64 trials, with each block lasting approximately 10 min. Subjects received feedback on the reaction time and stop rate after each block.

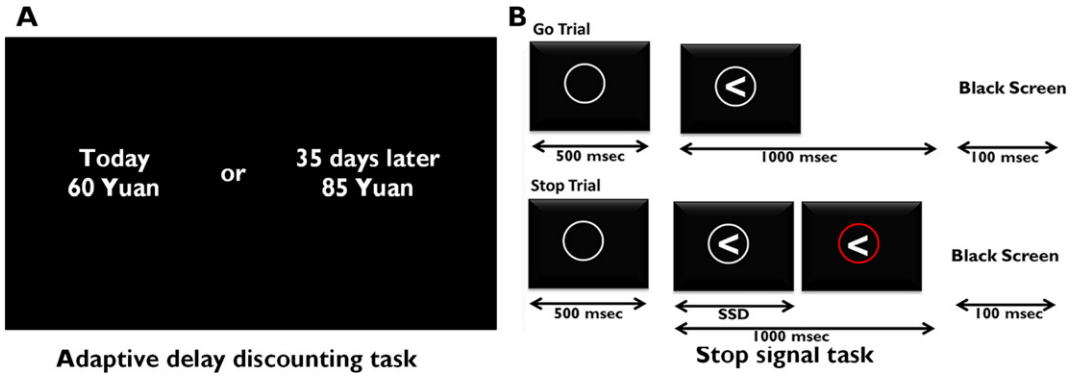

Fig. 1. The flow diagram of the experimental tasks. (A) The adaptive delay discounting task. During each trial, a fixed immediate reward (SS, RMB 60 paid today) and a varied delayed reward (LL, RMB 78–108 to be paid in 15 to 45 days) were simultaneously presented on the screen (the task was in Chinese, but shown above in English translation). The initial discounting factor was set to 0.02 and was increased or decreased when the participants chose the SS or LL option, respectively. For the first 20 trials (out of the total 60 trials), the step size for changes of k (delay discounting rate) was set to 0.01 and after that the step size decreased by 5% for each following step. (B) The stop-signal task. During each trial, an arrow pointing left or right was displayed on the computer screen. For the Go trials, the participants were asked to respond as quickly and accurately as possible with a left or right key press (using the left or right index finger) in 1000 ms. For the Stop trials, a stop signal (red circle) appeared at a stop-signal delay (SSD) subsequent to the arrow stimulus, and participants were asked to withhold the response they already initiated.

2.3. Behavioral data analysis

Statistical analyses of the behavioral data were performed using MATLAB (MathWorks, Natick, MA, USA). For impulsive choice, we used the multidimensional unconstrained nonlinear minimization function (fminsearch) of the optimization toolbox implemented in MATLAB for model fitting. Hyperbolic function ($SV = A / (1 + k * D)$) was used to compute the subjective value. To model trial-by-trial choices, we used a softmax function to compute the probability of choosing the immediate option (P_{SS}) on trial *t* as a function of the difference in V_{SS} and V_{LL}: $P_{SS} = 1 / (1 + \exp(-1 * m * (V_{SS} - V_{LL})))$, where m is the decision slope. Individual discounting rates were determined as the value k that maximized the likelihood of the observed choices. Because the distribution of the raw delay discounting rates was not normal, we used log-transformed k to represent impulsive choice (log k) (van den Bos et al., 2014; van den Bos et al., 2015; Wang et al., 2014).

For impulsive action, stop-signal response time (SSRT) was analyzed following the procedure used in previous studies (Congdon et al., 2010; Congdon et al., 2012). First, mean SSD was calculated from the last five trials for each raw SSD, which guaranteed a stable SSD estimate. Then, all RTs for the correct Go trials (focusing on the last 124 trials) were arranged in ascending order, and the RT corresponding to the median trial was selected as the Go RT. SSRT was estimated by subtracting the mean SSD from the Go RT.

2.4. Brain imaging data acquisition

All structural and resting state functional MRI images were collected on a Siemens 3 T Trio scanner (Siemens Medical Systems, Erlangen, Germany). High-resolution T1-weighted structural images were acquired using a Magnetization Prepared Rapid Acquisition Gradient-Echo (MPRAGE) sequence: TR/TE = 1900 ms/2.52 ms; inversion time (TI) = 900 ms; flip angle = 9°; FOV = 256 × 256 mm^2; slices = 176; thickness = 1.0 mm; voxel size = 1 × 1 × 1 mm^3. Resting-state fMRI images were acquired using Gradient Echo type Echo Planar Imaging (GRE-EPI) sequence; TR/TE = 2000 ms/30 ms, flip angle = 90°, resolution matrix = 64 × 64, FOV = 220 × 220 mm^2, and thickness = 3 mm, slice gap = 1 mm, acquisition voxel size = 3.4 × 3.4 × 4 mm^3. A total of 32 slices were used to cover the whole brain. Each section contained 242 volumes. During the resting-state scanning, all subjects were instructed to relax and keep their eyes closed but not to sleep (Damoiseaux et al., 2006).

2.5. Structural MRI preprocessing

Structural MRI data were analyzed with the Oxford Centre for Functional MRI of the Brain (FMRIB) Software Library voxel-based morphometry (FSL-VBM), a VBM style analysis toolbox (Good et al., 2001) implemented in FSL. Brains from the structural images were extracted, tissue-type segmented, and then aligned to the gray-matter template in the MNI152 standard space. The spatially normalized images were then averaged to create a study-specific template, to which the native gray matter images were registered again using both linear and nonlinear algorithms. The registered partial volume images were then modulated by dividing them with the Jacobian of the warp field to correct for local expansion or contraction. The modulated segmented images, which represented the GMV, were then smoothed with an isotropic Gaussian kernel with 3 mm standard deviation.

2.6. Resting-state fMRI preprocessing

The resting-state fMRI data were preprocessed using Data Processing Assistant for Resting-State fMRI (DPARSF, http://resting-fmri.sourceforge.net/) implemented in the MATLAB (Math Works, Natick, MA, USA) platform. The first 10 volumes of each participant were discarded due to the magnetization disequilibrium and the participant's adaptation to the scanning noise. The remaining 232 volumes were slice-timing corrected and then realigned to the middle slice of the brain to correct for head motion. All realigned images were spatially normalized to the MNI template, resampled into 3 × 3 × 3 mm^3 resolution, and then smoothed with an isotropic 8 mm FWHM Gaussian kernel. White matter, cerebrospinal fluid, global signal, and six motion parameters for head movement were regressed out as nuisance variables to reduce the effects of head motion and non-neuronal BOLD fluctuations (Dai et al., 2014; Di Martino et al., 2008; Fox et al., 2005). Temporal filtering (0.01–0.08 Hz) and voxel-wise linear detrending also were applied to the resting-state fMRI data (Fox et al., 2009; Hacker et al., 2012; Shin et al., 2014).

2.7. Resting-state functional connectivity analysis

To examine the resting-state functional connectivity, two seed regions were defined based on the VBM results in the current study, as well as existing functional imaging studies. Specifically, the right frontal pole (FP) (MNI = 16, 40, 38, radius = 5 mm), where the GMV significantly predicted individuals' k, was defined as the seed region for

impulsive choice. This region has also been implicated in representing delayed reward in existing imaging studies (Luhmann et al., 2008; Wang et al., 2014). In contrast, the right IFG (MNI = 54, 18, 22, radius = 5 mm), where the GMV significantly predicted individuals' SSRT, was defined as the seed region for impulsive action. This region has also been implicated in response inhibition (Aron et al., 2003; Tabibnia et al., 2011). Seed-based resting-state functional connectivity maps were produced by extracting the BOLD time course from a seed region and then computing the correlation coefficients between that time course and the time courses from all other brain voxels. The correlation coefficients were converted to a normal distribution through Fisher's z transform and then used for further analysis.

Group-level analyses were performed by using a mixed-effects model (FLAME) implemented in FSL. To control the effect of head motion, participants' mean frame-wise displacements (FD) were included as a covariate (Yan et al., 2013). This produced averaged functional connectivity maps associated with impulsive choice and impulsive action, as well as their direct comparisons. Corrections for multiple comparisons were carried out at the cluster level using Gaussian random field theory (min $z > 2.3$; cluster significance: $p < 0.01$, corrected).

2.8. Correlation with behavioral performance using MVPA

The preprocessed VBM imaging data and RSFC data were used to predict individual k and SSRT using an Epsilon-insensitive support vector regression (SVR) (Drucker et al., 1997) with a linear kernel, as implemented in PyMVPA (Multivariate Pattern Analysis in Python; http://www.pymvpa.org/; (Hanke et al., 2009)). A searchlight procedure with a three-voxel radius (Kriegeskorte et al., 2006) was used to provide a measure of decoding accuracy in the neighborhood of each voxel. Following Jimura and Poldrack (2012) and He et al. (2013), we set the ε parameter in the SVR to be 0.01.

A ten-fold cross-validation was applied. The 227 participants were divided into 10 groups of 22 or 23 participants, with matched gender as well as matched k or SSRT, depending on the specific analysis. In each iteration, an SVR model was trained based on 203 or 204 participants. Once trained, this SVR model then generated a prediction from the score of the excluded 22 or 23 participants based on their imaging data. Voxelwise accuracy of SVR prediction was then calculated as the Pearson's correlation coefficient between actual and predicted values of the k (or SSRT). Similarly, we used the searchlight approach and the same parameters to decode k or SSRT based on the RSFC z-maps. To control the effect of motion on RSFC, individuals' mean FDs were first regressed out and the residuals were subjected to SVR. Then, SVR predictions were thresholded using cluster detection statistics, with a height threshold of $z > 0.138$ (which corresponds to $r = 0.1386$, $p = 0.05$, uncorrected) and a cluster probability of $p < 0.05$, corrected for whole-brain multiple comparisons using Gaussian random field theory. Direct comparisons of the prediction accuracy of k and that of SSRT were conducted using Fisher r-to-z transformation.

2.9. Univariate correlational analysis

To further probe the direction of the association between GMV or RSFC and k or SSRT, we chose the clusters showing significantly different prediction accuracies of k and SSRT as ROIs. The averaged GMV or RSFC were then extracted and correlated (Pearson's) with k and SSRT after controlling for the mean FD. After controlling the age and gender, the results remained largely unchanged, suggesting that our results were not confounded by these factors. In order to avoid the double dipping issue, we only reported the positive and negative direction of correlation, but not the exact r or p value.

3. Results

3.1. Behavioral results

For the impulsive choice task, the hyperbolic function and the softmax function could accurately predict 76% (SD 11%) of the choices. The mean discounting rate estimated from this model was 0.021 ± 0.021, which was consistent with previous studies. For the stop signal task, the averaged Go RT and SSD were 445.8 ± 57.2 and 216.7 ± 74.2 ms, respectively, which were also consistent with previous studies. Critically, the averaged success rates of the Go trials and Stop trials in the stop signal task were 97% and 50.6%, respectively, indicating that the staircase procedure adequately tracked the behavioral performance. The distributions of impulsive choice performance (Kolmogorov–Smirnov $z = 0.88$, $p = 0.41$) and impulsive action performance (Kolmogorov–Smirnov $z = 1.12$, $p = 0.16$) were normal in our sample (Fig. 2A and B). No gender differences were found for impulsive choice ($t = 0.57$, $p = 0.57$) or impulsive action ($t = 1.16$, $p = 0.25$), but there were significant correlations between k and age ($r = -0.13$, $p = 0.04$), and between SSRT and age ($r = 0.18$, $p = 0.006$).

More importantly, correlational analysis revealed that impulsive choice and impulsive action were not significantly correlated, using either the linear function ($r = -.05$, $p > 0.05$) (Fig. 2C), or nonlinear functions, such as exponential ($F = 0.623$, $p = 0.431$), inverse ($F = 0.792$, $p = 0.374$), quadratic ($F = 0.577$, $p = 0.563$), cubic ($F = 0.427$, $p = 0.734$), or S-shape ($F = 0.685$, $p = 0.409$) function. These results suggested that these two tasks measured different aspects of impulsivity.

3.2. VBM results

Using MVPA, we found that k could be successfully predicted by the GMVs in the right frontal pole (FP; MNI = 16, 40, 38, prediction accuracy $r = 0.236$) and left middle frontal gyrus (MFG; MNI = −50, 34, 34, $r = 0.194$) (Fig. 3A). Other brain regions showing similar predictive accuracy included the left orbitofrontal cortex (OFC; MNI = −10, 20, −18, $r = 0.167$), right parahippocampus (PH; MNI = 20, −24, −36, $r = 0.225$), left putamen (MNI = −28, −12, 12, $r = 0.206$), right precentral gyrus (PG; MNI = 44, −6, 40, $r = 0.214$), left temporal pole (TP; MNI = −62, 12, −4, $r = 0.192$), and precuneus (MNI = 0, −68, 66, $r = 0.198$) (Table 1). Direct comparison revealed a significantly larger positive correlation for k than for SSRT in the FP ($z = 2.7$, $p < 0.01$) and MFG ($z = 2.68$, $p < 0.01$). To probe the direction of the association between ROIs' GMVs and k, a further correlational analysis found that k was positively associated with the GMVs in the FP and MFG (Fig. 3C). In contrast, these ROIs' GMVs were not correlated with SSRT (Fig. 3B).

The SSRT could be successfully predicted by the GMVs in the right inferior frontal gyrus (IFG; MNI = 54, 18, 22, $r = 0.201$), supplementary motor area (SMA; MNI = 0, 2, 58, $r = 0.168$), and anterior cingulate cortex (ACC; MNI = 2, 34, 14, $r = 0.181$) (Fig. 4A). Other brain regions showing similar predictive accuracy included the right insula (MNI = 44, 6, −12, $r = 0.246$), left precentral gyrus (MNI = −44, −10, 44, $r = 0.216$), left PH (MNI = −10, 0, −24, $r = 0.204$), right occipital fusiform gyrus (MNI = 12, −74, −22, $r = 0.171$), left MFG (MNI = −36, 24, 58, $r = 0.185$), and left lingual gyrus (LG; MNI = −8, −62, 0, $r = 0.195$) (Table 2). Direct comparison revealed significantly larger correlations for SSRT than for k in the IFG ($z = 2.01$, $p < 0.05$), ACC ($z = 1.98$, $p < 0.05$) and SMA ($z = 2.22$, $p < 0.05$). To probe the direction of the association between ROIs' GMVs and SSRT, further correlational analyses found that SSRT was positively correlated with the GMVs in the IFG and SMA, but negatively associated with the GMV in the ACC (Fig. 4B), but the GMVs in these regions showed no significant correlation with k (Fig. 4C). These results clearly suggested dissociated neuroanatomical correlates of impulsive choice and impulsive action.

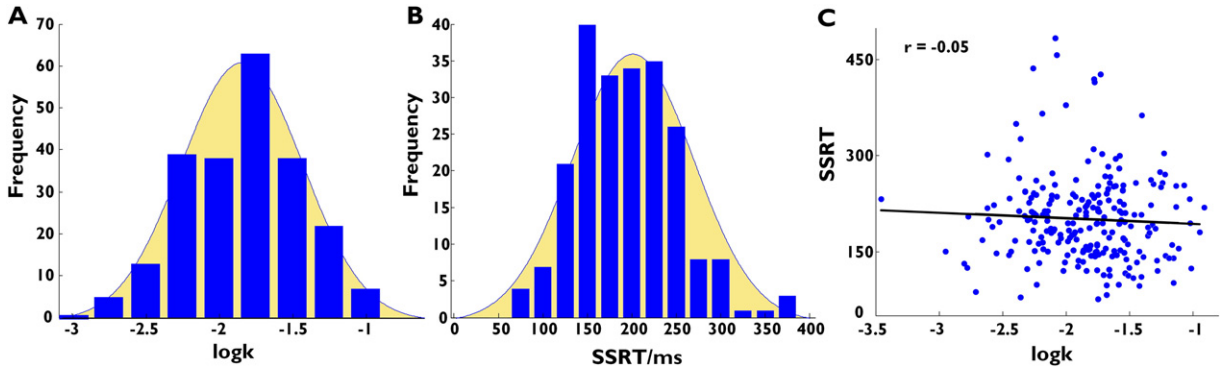

Fig. 2. The distributions of individuals' delay discounting rates (log k) (A) and response inhibition scores (SSRT) (B), and their correlation (C).

3.3. RSFC network using the right FP and IFG as seeds

Using the right FP as the seed region to identify the network for impulsive choice, we found a network of the MPFC, PCC, medial and lateral OFC, ventral striatum, and medial temporal lobule (Fig. 5A). In contrast, using the right IFG as the seed region to identify the network for impulsive action, we found a network that included the AI, SMG, dorsal ACC, pre-SMA, and thalamus (Fig. 5B). Direct comparisons between the two networks revealed stronger functional connectivity with the right FP seed than the right IFG in the VMPFC, PCC, medial temporal, hippocampus, VS, and thalamus; and stronger functional connectivity with the right IFG seed than the right FP in the ACC, pre-SMA, insula, LPFC, IPL, and SMG (Fig. 5C).

3.4. RSFC's associations with impulsive choice and impulsive action

We further examined whether distinct functional networks predicted k and SSRT. Using MVPA on the seed-based RSFC map, we found that individuals' k could be successfully predicted by the RSFC between the FP seed region and the ventromedial prefrontal cortex (VMPFC; MNI = −8, 30, −6, prediction accuracy $r = 0.21$) (Fig. 6A). Other brain regions showing similar predictive accuracy included the right ventral striatum (VS; MNI = 6, 4, 2, $r = 0.268$), right anterior PFC (MNI = 26, 42, 42, $r = 0.29$), left lateral prefrontal cortex (MNI = −46, −54, −6, $r = 0.174$), right SMG (MNI = 52, −34, 42, $r = 0.215$), left SMG (MNI = −62, −36, 48, $r = 0.219$), left SFG (MNI = −16, 10, 54, $r = 0.244$), right postcentral gyrus (MNI = 16, −36, 70, $r = 0.194$), left precentral gyrus (MNI = −54, −4, 38, $r = 0.19$), right precuneus (MNI = 4, −60, 66, $r = 0.196$), right LOC (MNI = 48, −66, 4, $r = 0.225$), right OP (MNI = 8, −90, 18, $r = 0.241$), and lingual gyrus (LG; MNI = −18, −54, −6, $r = 0.172$) (Table 3). Direct comparison revealed a significantly larger correlation for k than for SSRT in the VMPFC ($z = 2.21$, $p < 0.05$). To probe the direction of the association between seeds-based RSFC and k, further correlational analyses indicated that RSFC between FP seed and VMPFC region (Fig. 6C) was negatively correlated with k but not with SSRT (Fig. 6B).

Using the right IFG as the seed region, we found that SSRT could be predicted by the RSFC between the right IFG and the pre-SMA (MNI = 6, 18, 46, $r = 0.20$) (Fig. 6A). Other brain regions showing similar predictive accuracy included the right LOC (MNI = 40, −78, 24, $r = 0.176$), right superior temporal gyrus (STG; MNI = 68, −6, −8, $r = 0.199$), and right cerebellum (MNI = 30, −74, −38, $r = 0.171$) (Table 4). Direct comparison revealed a significantly larger correlation for SSRT than for k in the pre-SMA ($z = 2.03$, $p < 0.05$). To probe the direction of the association between seeds-based RSFC and SSRT, further correlational analyses suggested that RSFC between IFG and pre-SMA was negatively associated with SSRT (Fig. 6B), but no significant correlation was found for k (Fig. 6C). These RSFC results further showed evidence of dissociated substrates of impulsive choice and impulsive action.

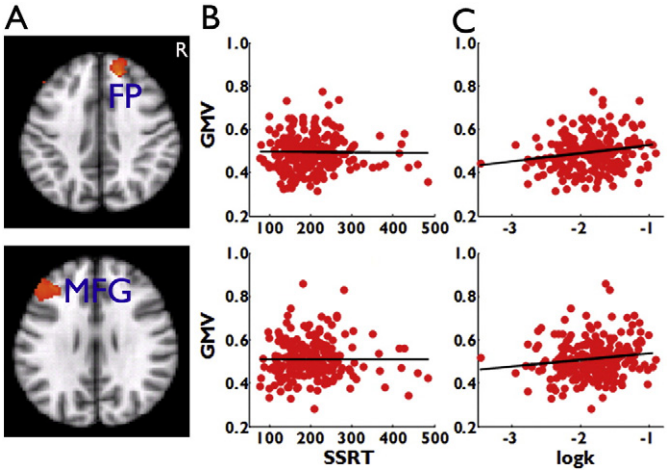

Fig. 3. VBM's MVPA and univariate results on the relationship between GMV and delay discounting. (A) shows regions where the GMV predicted individuals' k using MVPA. (B) and (C) show the correlations between GMV and SSRT and k, respectively. FP, frontal pole; MFG, middle frontal gyrus.

4. Discussion

Using a relatively large sample, two well-validated cognitive tasks, and a cross-validation approach on the GMV and RSFC data, the present study investigated whether there were distinct or common neural networks for impulsive choice and impulsive action. Several results suggest that impulsive choice and impulsive action reflect different aspects of impulsivity and are supported by dissociated neural networks. First, at the behavioral level, our results showed that impulsive choice and impulsive action were independent. Second, at the neuroanatomical level, we found that the GMVs in the FP and MFG were associated with impulsive choice, whereas the GMVs in the IFG, SMA, and ACC

Table 1
Brain regions showing significant correlations between gray matter volume (GMV) and impulsive choice in multivariate pattern analysis.

Brain regions	L/R	No. voxels	MNI coordinates			Prediction accuracy (r)
			x	y	z	
Frontal pole	R	227	16	40	38	0.236
Middle frontal gyrus	L	527	−50	34	34	0.194
Orbitofrontal cortex	L	239	−10	20	−18	0.167
Parahippocampus	R	1053	20	−24	−36	0.225
Putamen	L	244	−28	−12	12	0.206
Precentral	R	583	44	−6	40	0.214
Temporal pole	L	418	−62	12	−4	0.192
Precuneus	L/R	289	0	−68	66	0.198

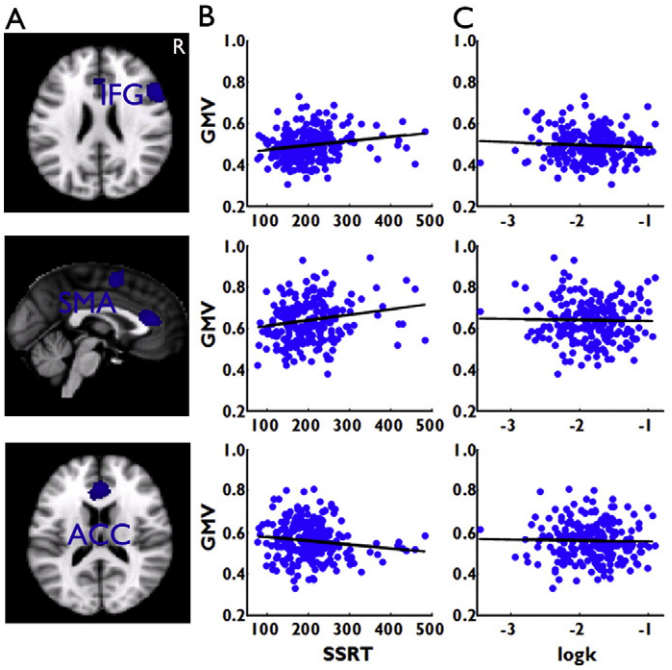

Fig. 4. VBM's MVPA and univariate results on the relationship between GMV and response inhibition. (A) shows regions whose GMVs could predict individuals' SSRT using MVPA. (B) and (C) show the correlations between GMV and SSRT and k, respectively. IFG, inferior frontal gyrus; SMA, supplementary motor area; ACC, anterior cingulate cortex.

were associated with impulsive action. Third, we found that the FP and the right IFG were part of dissociated functional networks that have been implicated in different aspects of impulsivity. Finally, we found that RSFC between the FP and the VMPFC could successfully predict the impulsive choice performance, whereas RSFC between the right IFG and the pre-SMA predicted the impulsive action performance.

Our results were consistent with previous functional imaging findings that the FP, MFG, and VMPFC were involved in delay discounting (Kable and Glimcher, 2007; McClure et al., 2007; McClure et al., 2004; Peters and Büechel, 2011; Wang et al., 2014). In particular, our results provided additional evidence to support the critical role of the frontal pole (including the anterior DMPFC) in delay discounting (Wang et al., 2014). Sitting at the top of the posterior–anterior hierarchy of the prefrontal cortex, the frontal pole has been implicated in high-level control (Ramnani and Owen, 2004; Venkatraman et al., 2009) and exploratory decision (Daw et al., 2006), and is responsible for processing information conveying delay in the future, low certainty, or less tangibility (Bechara and Damasio, 2005).

Consistently, previous studies have suggested that the anterior DMPFC was more involved in processing temporally distant reward than temporally proximate reward (Koritzky et al., 2013). It showed greater activation in the delay condition than in the immediate condition (Luhmann et al., 2008) and supported farsighted decision (Benoit et al., 2011). Moreover, activation in this region predicted individuals' trait impulsivity as measured by the Barratt Impulsiveness Scale (Sripada et al., 2011). Finally, high-frequency TMS on MPFC was found to decrease the delay discounting rate and the magnitude of change was associated with TMS-induced release of DA in the dorsal striatum (Cho et al., 2014).

Our functional connectivity results suggested that the frontal pole may contribute to intertemporal choice via two important connections. First, the FP showed strong functional connectivity with the hippocampus, which has been implicated in episodic future thinking (Schacter et al., 2007), and is posited to modulate intertemporal choice (Lebreton et al., 2013; Peters and Büchel, 2010) and to reduce impulsivity (Daniel et al., 2013) (also see Lucci, 2013 for a review). It is thus conceivable that through the FP–hippocampus connection, the hippocampus can modulate the value representation in the DMPFC and frontal pole. Consistent with this view, it is suggested that the FP represents the overall anticipated affective quality, thus enabling the prediction of future value (Benoit et al., 2014). During intertemporal choice, activation in this region reflected the reward magnitude of imagined episodes, and less discounting was associated with increased mrPFC–hippocampal coupling (Benoit et al., 2011).

Second, the FP may modulate the decision value representation in the VMPFC that is linked to behavioral choice (Bartra et al., 2013; Clithero and Rangel, 2014). Many studies have shown that the VMPFC represents reference-dependent value signal (FitzGerald et al., 2009; Hare et al., 2008; Knutson et al., 2007; Lim et al., 2011; Plassmann et al., 2007; Sripada et al., 2011; Wang et al., 2014), regardless of the categories of goods presented or the specific types of comparison being performed (Chib et al., 2009; FitzGerald et al., 2009; McNamee et al., 2013). We found that a strong functional connectivity between the FP and VMPFC was associated with less discounting, suggesting that the FP upregulated the value representation of the delayed value and resulted in more patient decisions.

The role of lateral prefrontal cortex in impulsive choice remains inconclusive. Previous studies have found that the structural and functional connectivity between right DLPFC and VS predicted individuals' impulsive choice (van den Bos et al., 2014), whereas the current study found that the GMV in the left DLPFC was associated with impulsive choice. Similarly, brain stimulation studies also found inconsistent results regarding the role of left or right DLPFC in intertemporal choice. For example, whereas one study found that TMS on left DLPFC, but not right DLPFC, increased choices of immediate rewards over larger delayed rewards (Figner et al., 2010), another study found that TMS on the right DLPFC increased choices of immediate rewards (Essex et al., 2012). A tDCS study found that when the left DLPFC was facilitated and the right DLPFC inhibited, participants chose smaller immediate gains (Hecht et al., 2013). Future studies should further examine the role of the left vs. right DLPFC in impulsive choice.

We also found that the GMVs in the right IFG, SMA, and ACC were associated with impulsive action. Functional imaging studies have consistently implicated these regions in impulsive action as measured by the stop-signal task (Aron et al., 2014; Congdon et al., 2008; White et al., 2014). In particular, a recent study of functional connectivity and impulsive action showed that the right IFG and pre-SMA were involved in response inhibition, whereas the ACC and insula were important for detecting the salient stimuli (Cai et al., 2014). Also consistent with several previous observations emphasizing the connectivity of rIFG and pre-SMA in response inhibition (Aron et al., 2007a; Duann et al., 2009; Swann et al., 2012), we found that the RSFC between the right IFG seed region and pre-SMA predicted impulsive action performance.

A growing number of studies have suggested that response inhibition can be achieved via at least two mechanisms, a reactive inhibitory control mechanism that is cued by the stop signal and acts on the stop

Table 2
Brain regions showing significant correlations between GMV and impulsive action in multivariate pattern analysis.

Brain regions	L/R	No. voxels	MNI coordinates			Prediction accuracy (r)
			x	y	z	
Inferior frontal gyrus	R	773	54	18	22	0.201
Supplementary motor area	L/R	361	0	2	58	0.168
Anterior cingulate cortex	R	501	2	34	14	0.181
Insula	R	1436	44	6	−12	0.246
Precentral gyrus	L	881	−44	−10	44	0.216
Parahippocampus gyrus	L	602	−10	0	−24	0.204
Occipital fusiform gyrus	R	368	12	−74	−22	0.171
Middle frontal gyrus	L	244	−36	24	58	0.185
Lingual gyrus	L	249	−8	−62	0	0.195

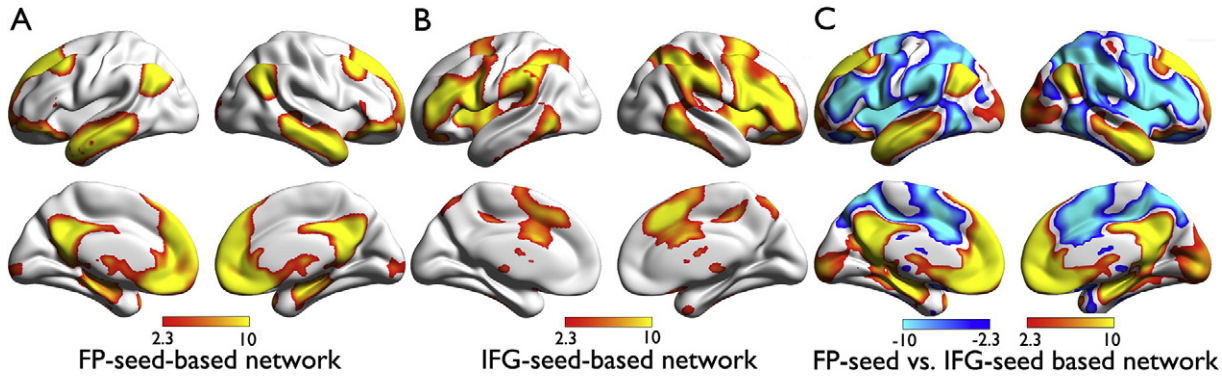

Fig. 5. Resting-state functional networks associated with the FP and IFG seed regions. (A) The FP-seed-based network and (B) the IFG-seed-based network were computed by *t*-test and were compared with each other (C). Red color indicates stronger functional connectivity with the right FP seed than with the right IFG, whereas blue color indicates stronger functional connectivity with the right IFG seed than with the right FP seed.

process, and a memory-related proactive inhibitory control mechanism that acts on the go process (Aron, 2011). Although the current study suggests that the rIFG and pre-SMA network is involved in reactive inhibitory process, the same network has also been implicated in proactive inhibitory control (Chikazoe et al., 2009; Jahfari et al., 2011; Swann et al., 2012; White et al., 2014). In particular, a recent transcranial current stimulation study showed that anodal stimulation of the right IFG enhanced both reactive and proactive inhibitory control (Cai et al., 2015).

Recent studies suggest that stop-signal detection and the implementation of stopping might be supported by different subregions of the right IFG. For example, a TMS study showed that the dorsal-posterior and ventral-posterior parts of the right IFG were involved in responding to infrequent stop signals and in triggering the actual stop process, respectively (Verbruggen et al., 2010). Consistently, previous neuroimaging studies showed that, whereas the pre-SMA was involved in response inhibition (Chao et al., 2009; Li et al., 2006), ventral IFG was involved in post-conflict and post-error behavioral adjustment (Li et al., 2008). However, other studies suggested that the right IFG was also involved in the detection of stop signals (Chikazoe et al., 2009; Erika-Florence et al., 2014; Hampshire et al., 2010; Sharp et al., 2010), the change of stimulus–reward contingency (Mullette-Gillman and Huettel, 2009; Xue et al., 2013), and other infrequent salient events (Erika-Florence et al., 2014), all of which are important for response inhibition. Future studies should further examine the role of DLPFC subregions in response inhibition.

The RSFC networks based on the FP seed and rIFG seed correspond very well to the "Waiting" impulsivity and "Stopping" impulsivity networks proposed by Dalley et al. (2011). In particular, the infralimbic and prelimbic prefrontal cortex, hippocampus, amygdala, and ventral striatum are included in the "Waiting" impulsivity network, whereas the rIFG/OFC, pre-SMA, and dorsal striatum are included in the "Stopping" impulsivity network. Intriguingly, this contrast between the medial "Waiting" system and lateral "Stopping" system seems to fit well to the contrast between the "hot" affective vs. "cold" cognitive systems of executive function suggested by a large body of research (Kerr and Zelazo, 2004; Metcalfe and Mischel, 1999; Zelazo and Carlson, 2012). Our RSFC results suggest that these two systems might be rooted in the fundamental neural architectures of the brain. Future studies should further examine, at the neural network level, how different aspects of executive controls are supported by dissociated neural networks.

It should be noted that we observed that greater GMVs in the FP and right IFG were associated with greater discounting rates and worse inhibitory control, respectively, whereas those in the OFC, ACC and insula were positively correlated with impulsive behaviors. Meanwhile, we found that greater FP–VMPFC and IFG–pre-SMA functional connectivity were associated with lower discounting rates and better inhibitory control. This structural and functional dissociation is very consistent with the developmental trajectory of human brain (Shaw et al., 2006; Sowell et al., 1999). In particular, unlike the posterior brain regions that mature rapidly between childhood and adolescence, the structural and functional maturation of the prefrontal cortex, as marked by gray matter loss (Casey et al., 2005; Caviness et al., 1999; Reiss et al., 1996)

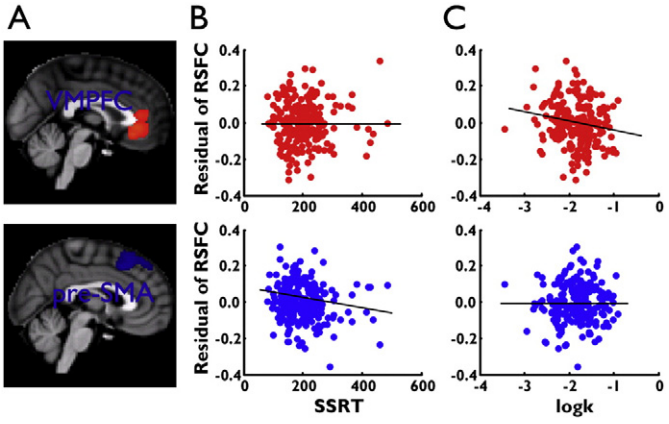

Fig. 6. MVPA and univariate results on the relationship between resting-state functional connectivity for the FP and IFG seeds and task performance (SSRT and k). (A) MVPA revealed that the resting-state functional connectivity (RSFC) between the FP and VMPFC was predictive of individuals' k, whereas the RSFC between the IFG and pre-SMA was predictive of individuals' SSRT. (B) shows the correlation between the residuals of RSFC and k after controlling for the head motion. (C) shows the correlation between the residuals of RSFC and SSRT after controlling for the head motion.

Table 3
Brain regions showing significant correlations between RSFC of the FP seed and impulsive choice in multivariate pattern analysis.

Brain regions	L/R	No. voxels	MNI coordinates			Prediction accuracy (*r*)
			x	y	z	
Ventromedial prefrontal cortex	L	1171	−8	30	−6	0.21
Ventral striatum	R	2300	6	4	2	0.268
Anterior prefrontal cortex	R	2789	26	42	42	0.29
Lateral prefrontal cortex	L	1221	−46	−54	−6	0.174
Supramarginal gyrus	R	1325	52	−34	42	0.215
Supramarginal gyrus	L	1005	−62	−36	48	0.219
Superior frontal gyrus	L	472	−16	10	54	0.244
Precuneus	R	510	4	−60	66	0.196
Postcentral	R	250	16	−36	70	0.194
Precentral	L	405	−54	−4	38	0.19
Lateral occipital cortex	R	365	48	−66	4	0.225
Occipital pole	R	2694	8	−90	18	0.241
Lingual gyrus	L	293	−18	−54	−6	0.174

Table 4
Brain regions showing significant correlations between RSFC of the IFG seed and impulsive action in multivariate pattern analysis.

Brain regions	L/R	No. voxels	MNI coordinates			Prediction accuracy (r)
			x	y	z	
Presupplementary motor area	R	680	6	18	46	0.20
Superior temporal gyrus	R	298	68	−6	−8	0.199
Lateral occipital cortex	R	238	40	−78	24	0.176
Cerebellum	R	272	30	−74	−38	0.171

and cortical thinning (Lu et al., 2009; Sowell et al., 1999), will continue until young adulthood (Sowell et al., 1999). Within the prefrontal cortex, phylogenetically older brain areas mature earlier than do newer areas (Gogtay et al., 2004). As a result, the inversed relationship between the GMVs in the phylogenetically older regions (i.e., ACC, OFC and Insula) and those in the newer regions (i.e., IFG, FP) might reflect their differential developmental trajectories. Nevertheless, due to the complex relations between brain structural development, brain function, and impulsive behaviors, future studies should use both functional MRI and longitudinal studies to examine their causal relations.

Findings of this study have important implications for the study of clinical populations with impulsive symptoms, such as addiction, ADHD, and antisocial behaviors. In particular, a deeper understanding of the multifaceted construct of impulsivity should provide an important theoretical framework to better characterize the core deficits associated with different clinical populations. For this purpose, it would be fruitful for future studies to examine whether different clinical populations are impaired in particular aspects of executive control, using large-scale meta-analysis (Poldrack et al., 2012) as well as direct comparisons (Moeller et al., 2001). These results should help to reveal the core impulsivity endophenotype, which has significant implications for the understanding of the ontology, etiology, development, and treatment of impulsive disorders.

Acknowledgment

We thank Samuel McClure for sharing the adaptive delayed discounting task and analysis script. This work was sponsored by the National Natural Science Foundation of China (31130025), the 973 Program (2014CB846102), the 111 Project (B07008), and the NSFC project (31221003).

References

Ainslie, G., 1975. Specious reward: a behavioral theory of impulsiveness and impulse control. Psychol. Bull. 82 (4), 463.
Alessi, S., Petry, N., 2003. Pathological gambling severity is associated with impulsivity in a delay discounting procedure. Behav. Process. 64 (3), 345–354.
Alexander, G., DeLong, M., Strick, P., 1986. Parallel organization of functionally segregated circuits linking basal ganglia and cortex. Annu. Rev. Neurosci. 9 (1), 357–381.
Aron, A., Poldrack, R., 2005. The cognitive neuroscience of response inhibition: relevance for genetic research in attention-deficit/hyperactivity disorder. Biol. Psychiatry 57 (11), 1285–1292.
Aron, A., Poldrack, R., 2006. Cortical and subcortical contributions to stop signal response inhibition: role of the subthalamic nucleus. J. Neurosci. 26 (9), 2424–2433.
Aron, A., Behrens, T., Smith, S., Frank, M., Poldrack, R., 2007a. Triangulating a cognitive control network using diffusion-weighted magnetic resonance imaging (MRI) and functional MRI. J. Neurosci. 27 (14), 3743–3752.
Aron, A., Durston, S., Eagle, D., Logan, G., Stinear, C., Stuphorn, V., 2007b. Converging evidence for a fronto-basal-ganglia network for inhibitory control of action and cognition. J. Neurosci. 27 (44), 11860–11864.
Aron, A., Robbins, T., Poldrack, R., 2004. Inhibition and the right inferior frontal cortex. Trends Cogn. Sci. 8 (4), 170–177.
Aron, A., Robbins, T., Poldrack, R., 2014. Inhibition and the right inferior frontal cortex: one decade on. Trends Cogn. Sci. 18 (4), 177–185.
Aron, A., 2011. From reactive to proactive and selective control: developing a richer model for stopping inappropriate responses. Biol. Psychiatry 69 (12), 55–68.
Aron, A.R., Fletcher, P.C., Bullmore, E.T., Sahakian, B.J., Robbins, T.W., 2003. Stop-signal inhibition disrupted by damage to right inferior frontal gyrus in humans. Nat. Neurosci. 6 (2), 115–116.
Bari, A., Robbins, T., 2013. Inhibition and impulsivity: behavioral and neural basis of response control. Prog. Neurobiol. 108, 44–79.
Barkley, R.A., 1997. Behavioral inhibition, sustained attention, and executive functions: constructing a unifying theory of ADHD. Psychol. Bull. 121 (1), 65–94.
Bartra, O., McGuire, J., Kable, J.W., 2013. The valuation system: a coordinate-based meta-analysis of BOLD fMRI experiments examining neural correlates of subjective value. NeuroImage 76, 412–427.
Bechara, A., Damasio, A., 2005. The somatic marker hypothesis: a neural theory of economic decision. Games Econ. Behav. 52 (2), 336–372.
Beck, A., Schlagenhauf, F., Wüstenberg, T., Hein, J., Kienast, T., Kahnt, T., Schmack, K., Hägele, C., Knutson, B., Heinz, A., 2009. Ventral striatal activation during reward anticipation correlates with impulsivity in alcoholics. Biol. Psychiatry 66 (8), 734–742.
Bednarski, S.R., Erdman, E., Luo, X., Zhang, S., Hu, S., Li, C.S.R., 2012. Neural processes of an indirect analog of risk taking in young nondependent adult alcohol drinkers—an fMRI study of the stop signal task. Alcohol. Clin. Exp. Res. 36 (5), 768–779.
Benoit, R., Gilbert, S., Burgess, P., 2011. A neural mechanism mediating the impact of episodic prospection on farsighted decisions. J. Neurosci. 31 (18), 6771–6779.
Benoit, R., Szpunar, K., Schacter, D., 2014. Ventromedial prefrontal cortex supports affective future simulation by integrating distributed knowledge. Proc. Natl. Acad. Sci. 111 (46), 16550–16555.
Bickel, W., Odum, A., Madden, G., 1999. Impulsivity and cigarette smoking: delay discounting in current, never, and ex-smokers. Psychopharmacology 146 (4), 447–454.
Billieux, J., Gay, P., Rochat, L., Khazaal, Y., Zullino, D., Van der Linden, M., 2010. Lack of inhibitory control predicts cigarette smoking dependence: evidence from a non-deprived sample of light to moderate smokers. Drug Alcohol Depend. 112 (1), 164–167.
Bjork, J., Momenan, R., Hommer, D., 2009. Delay discounting correlates with proportional lateral frontal cortex volumes. Biol. Psychiatry 65 (8), 710–713.
Broos, N., Schmaal, L., Wiskerke, J., Kostelijk, L., Lam, T., Stoop, N., Weierink, L., Ham, J., De Geus, E., Schoffelmeer, et al., 2012. The relationship between impulsive choice and impulsive action: a cross-species translational study. PLoS One 7 (5), e36781.
Cai, W., Ryali, S., Chen, T., Li, C., Menon, V., 2014. Dissociable roles of right inferior frontal cortex and anterior insula in inhibitory control: evidence from intrinsic and task-related functional parcellation, connectivity, and response profile analyses across multiple datasets. J. Neurosci. 34 (44), 14652–14667.
Cai, Y., Li, S., Liu, J., Li, D., Feng, Z., Wang, Q., Chen, C., Xue, G., 2015. The role of the frontal and parietal cortex in proactive and reactive inhibitory control: a transcranial direct current stimulation study. J. Cogn. Neurosci. 28 (1), 177–186.
Casey, B., Tottenham, N., Liston, C., Durston, S., 2005. Imaging the developing brain: what have we learned about cognitive development? Trends Cogn. Sci. 9 (3), 104–110.
Caviness, V.S., Lange, N.T., Makris, N., Herbert, M.R., Kennedy, D.N., 1999. MRI-based brain volumetrics: emergence of a developmental brain science. Brain Dev. 21 (5), 289–295.
Chambers, C., Garavan, H., Bellgrove, M., 2009. Insights into the neural basis of response inhibition from cognitive and clinical neuroscience. Neurosci. Biobehav. Rev. 33 (5), 631–646.
Chao, H., Luo, X., Chang, J., Li, C., 2009. Activation of the pre-supplementary motor area but not inferior prefrontal cortex in association with short stop signal reaction time—an intra-subject analysis. BMC Neurosci. 10 (1), 1–10.
Chib, V., Rangel, A., Shimojo, S., O'Doherty, J., 2009. Evidence for a common representation of decision values for dissimilar goods in human ventromedial prefrontal cortex. J. Neurosci. 29 (39), 12315–12320.
Chikazoe, J., Jimura, K., Hirose, S., Yamashita, K., Miyashita, Y., Konishi, S., 2009. Preparation to inhibit a response complements response inhibition during performance of a stop-signal task. J. Neurosci. 29 (50), 15870–15877.
Cho, S., Koshimori, Y., Aminian, K., Obeso, I., Rusjan, P., Lang, A., Daskalakis, Z., Houle, S., Strafella, A., 2014. Investing in the future: stimulation of the medial prefrontal cortex reduces discounting of delayed rewards. Neuropsychopharmacology 9, 1–8.
Clithero, J.A., Rangel, A., 2014. Informatic parcellation of the network involved in the computation of subjective value. Soc. Cogn. Affect. Neurosci. 9 (9), 1289–1302.
Congdon, E., Lesch, K., Canli, T., 2008. Analysis of DRD4 and DAT polymorphisms and behavioral inhibition in healthy adults: implications for impulsivity. Am. J. Med. Genet. B Neuropsychiatr. Genet. 147 (1), 27–32.
Congdon, E., Mumford, J., Cohen, J., Galvan, A., Aron, A., Xue, G., Miller, E., Poldrack, R., 2010. Engagement of large-scale networks is related to individual differences in inhibitory control. NeuroImage 53 (2), 653–663.
Congdon, E., Mumford, J., Cohen, J., Galvan, A., Canli, T., Poldrack, R., 2012. Measurement and reliability of response inhibition. Front. Psychol. 3, 1–10.
Coxon, J., Van Impe, A., Wenderoth, N., Swinnen, S., 2012. Aging and inhibitory control of action: cortico–subthalamic connection strength predicts stopping performance. J. Neurosci. 32 (24), 8401–8412.
Dai, Z., Yan, C., Li, K., Wang, Z., Wang, J., Cao, M., Lin, Q., Shu, N., Xia, M., Bi, Y., et al., 2014. Identifying and mapping connectivity patterns of brain network hubs in Alzheimer's disease. Cereb. Cortex 10, 1–20.
Dalley, J., Everitt, B., Robbins, T., 2011. Impulsivity, compulsivity, and top-down cognitive control. Neuron 69 (4), 680–694.
Damoiseaux, J., Rombouts, S., Barkhof, F., Scheltens, P., Stam, C., Smith, S., Beckmann, C., 2006. Consistent resting-state networks across healthy subjects. Proc. Natl. Acad. Sci. U. S. A. 103 (37), 13848–13853.
Daniel, T., Stanton, C., Epstein, L., 2013. The future is now reducing impulsivity and energy intake using episodic future thinking. Psychol. Sci. 24 (11), 2339–2342.
Daw, N., O'Doherty, J., Dayan, P., Seymour, B., Dolan, R., 2006. Cortical substrates for exploratory decisions in human. Nature 441 (7095), 876–879.

Dawe, S., Gullo, M., Loxton, N., 2004. Reward drive and rash impulsiveness as dimensions of impulsivity: implications for substance misuse. Addict. Behav. 29 (7), 1389–1405.
Di Martino, A., Scheres, A., Margulies, D., Kelly, A., Uddin, L., Shehzad, Z., Biswal, B., Walters, J., Castellanos, F., Milham, M., 2008. Functional connectivity of human striatum: a resting state FMRI study. Cereb. Cortex 18 (12), 2735–2747.
Donders, F.C., 1969. On the speed of mental processes. Acta Psychol. 30, 412–431.
Drucker, H., Burges, C., Kaufman, L., Smola, A., Vapnik, V., 1997. Support vector regression machines. Adv. Neural Inf. Proces. Syst. 9, 155–161.
Duann, J., Ide, J., Luo, X., Li, C., 2009. Functional connectivity delineates distinct roles of the inferior frontal cortex and presupplementary motor area in stop signal inhibition. J. Neurosci. 29 (32), 10171–10179.
Economides, M., Guitart-Masip, M., Kurth-Nelson, Z., Dolan, R., 2015. Arbitration between controlled and impulsive choice. NeuroImage 109, 206–216.
Erika-Florence, M., Leech, R., Hampshire, A., 2014. A functional network perspective on response inhibition and attentional control. Nat. Commun. 5, 1–12.
Essex, B., Clinton, S., Wonderley, L., Zald, D., 2012. The impact of the posterior parietal and dorsolateral prefrontal cortices on the optimization of long-term versus immediate value. J. Neurosci. 32 (44), 15403–15413.
Evenden, J., 1999. Varieties of impulsivity. Psychopharmacology 146 (4), 348–361.
Farr, O.M., Hu, S., Zhang, S., Chiang-shan, R.L., 2012. Decreased saliency processing as a neural measure of Barratt impulsivity in healthy adults. NeuroImage 63 (3), 1070–1077.
Figner, B., Knoch, D., Johnson, E., Krosch, A., Lisanby, S., Fehr, E., Weber, E., 2010. Lateral prefrontal cortex and self-control in intertemporal choice. Nat. Neurosci. 13 (5), 538–539.
Fillmore, M.T., Rush, C.R., 2002. Impaired inhibitory control of behavior in chronic cocaine users. Drug Alcohol Depend. 66 (3), 265–273.
FitzGerald, H., Seymour, B., Dolan, R., 2009. The role of human orbitofrontal cortex in value comparison for incommensurable objects. J. Neurosci. 29 (26), 8388–8395.
Forstmann, B., Keuken, M., Jahfari, S., Bazin, P., Neumann, J., Schäfer, A., Anwander, A., Turner, R., 2012. Cortico–subthalamic white matter tract strength predicts interindividual efficacy in stopping a motor response. NeuroImage 60 (1), 370–375.
Fox, M., Snyder, A., Vincent, J., Corbetta, M., Van Essen, D., Raichle, M., 2005. The human brain is intrinsically organized into dynamic, anticorrelated functional networks. Proc. Natl. Acad. Sci. U. S. A. 102 (27), 9673–9678.
Fox, M., Zhang, D., Snyder, A., Raichle, M., 2009. The global signal and observed anticorrelated resting state brain networks. J. Neurophysiol. 101 (6), 3270–3283.
Ghahremani, D., Lee, B., Robertson, C., Tabibnia, G., Morgan, A., De Shetler, N., Brown, A., Monterosso, J., Aron, A., Mandelkern, M., 2012. Striatal dopamine D2/D3 receptors mediate response inhibition and related activity in frontostriatal neural circuitry in humans. J. Neurosci. 32 (21), 7316–7324.
Gogtay, N., Giedd, J.N., Lusk, L., Hayashi, K.M., Greenstein, D., Vaituzis, A.C., Nugent, T.F., Herman, D.H., Clasen, L.S., Toga, A.W., 2004. Dynamic mapping of human cortical development during childhood through early adulthood. Proc. Natl. Acad. Sci. U. S. A. 101 (21), 8174–8179.
Good, C., Johnsrude, I., Ashburner, J., Henson, R., Friston, K., Frackowiak, R., 2001. Cerebral asymmetry and the effects of sex and handedness on brain structure: a voxel-based morphometric analysis of 465 normal adult human brains. NeuroImage 14 (3), 685–700.
Hacker, C., Perlmutter, J., Criswell, S., Ances, B., Snyder, A., 2012. Resting state functional connectivity of the striatum in Parkinson's disease. Brain 135 (12), 1–13.
Hampshire, A., Sharp, D.J., 2015. Contrasting network and modular perspectives on inhibitory control. Trends Cogn. Sci. 19 (8), 445–452.
Hampshire, A., Chamberlain, S., Monti, M., Duncan, J., Owen, A., 2010. The role of the right inferior frontal gyrus: inhibition and attentional control. NeuroImage 50 (3), 1313–1319.
Hanke, M., Halchenko, Y., Sederberg, P., Hanson, S., Haxby, J., Pollmann, S., 2009. PyMVPA: a python toolbox for multivariate pattern analysis of fMRI data. Neuroinformatics 7 (1), 37–53.
Hare, R.D., Neumann, C., 2008. Psychopathy as a clinical and empirical construct. Annu. Rev. Clin. Psychol. 4, 217–246.
Hare, T., Camerer, C., Rangel, A., 2009. Self-control in decision-making involves modulation of the vmPFC valuation system. Science 324 (5927), 646–648.
Hare, T., O'Doherty, J., Camerer, C., Schultz, W., Rangel, A., 2008. Dissociating the role of the orbitofrontal cortex and the striatum in the computation of goal values and prediction errors. J. Neurosci. 28 (22), 5623–5630.
Hariri, A., Brown, S., Williamson, D., Flory, J., de Wit, H., Manuck, S., 2006. Preference for immediate over delayed rewards is associated with magnitude of ventral striatal activity. J. Neurosci. 26 (51), 13213–13217.
He, Q., Xue, G., Chen, C., Chen, C., Lu, Z., Dong, Q., 2013. Decoding the neuroanatomical basis of reading ability: a multivoxel morphometric study. J. Neurosci. 33 (31), 12835–12843.
Hecht, D., Walsh, V., Lavidor, M., 2013. Bi-frontal direct current stimulation affects delay discounting choices. Cogn. Neurosci. 4 (1), 7–11.
Hu, S., Ide, J.S., Zhang, S., Sinha, R., Chiang-shan, R.L., 2015. Conflict anticipation in alcohol dependence—a model-based fMRI study of stop signal task. NeuroImage Clin. 8, 39–50.
Jahfari, S., Waldorp, L., van den Wildenberg, W., Scholte, H., Ridderinkhof, K., Forstmann, B., 2011. Effective connectivity reveals important roles for both the hyperdirect (fronto-subthalamic) and the indirect (fronto-striatal-pallidal) fronto-basal ganglia pathways during response inhibition. J. Neurosci. 31 (18), 6891–6899.
Jimura, K., Poldrack, R.A., 2012. Analyses of regional-average activation and multivoxel pattern information tell complementary stories. Neuropsychologia 50, 544–552.
Johnson, M.W., Bickel, W.K., 2002. Within-subject comparison of real and hypothetical money rewards in delay discounting. J. Exp. Anal. Behav. 77 (2), 129–146.
Kable, J., Glimcher, P., 2007. The neural correlates of subjective value during intertemporal choice. Nat. Neurosci. 10 (12), 1625–1633.
Kable, J., Glimcher, P., 2009. The neurobiology of decision: consensus and controversy. Neuron 63 (6), 733–745.
Kerr, A., Zelazo, P., 2004. Development of "hot" executive function: the children's gambling task. Brain Cogn. 55 (1), 148–157.
Kirby, K., Petry, N., Bickel, W., 1999. Heroin addicts have higher discount rates for delayed rewards than non-drug-using controls. J. Exp. Psychol. Gen. 128 (1), 78–87.
Knutson, B., Rick, S., Wimmer, G., Prelec, D., Loewenstein, G., 2007. Neural predictors of purchases. Neuron 53 (1), 147–156.
Koritzky, G., He, Q., Xue, G., Wong, S., Xiao, L., Bechara, A., 2013. Processing of time within the prefrontal cortex: recent time engages posterior areas whereas distant time engages anterior areas. NeuroImage 72, 280–286.
Kriegeskorte, N., Goebel, R., Bandettini, P., 2006. Information-based functional brain mapping. Proc. Natl. Acad. Sci. U. S. A. 103 (10), 3863–3868.
Lagorio, C.H., Madden, G.J., 2005. Delay discounting of real and hypothetical rewards III: steady-state assessments, forced-choice trials, and all real rewards. Behav. Process. 69 (2), 173–187.
Lansbergen, M., Böcker, K., Bekker, E., Kenemans, J., 2007. Neural correlates of stopping and self-reported impulsivity. Clin. Neurophysiol. 118 (9), 2089–2103.
Lebreton, M., Bertoux, M., Boutet, C., Lehericy, S., Dubois, B., Fossati, P., Pessiglione, M., 2013. A critical role for the hippocampus in the valuation of imagined outcomes. PLoS Biol. 11 (10), e1001684.
Li, C., Chao, H.H.-A., Lee, T.-W., 2009. Neural correlates of speeded as compared with delayed responses in a stop signal task: an indirect analog of risk taking and association with an anxiety trait. Cereb. Cortex 19 (4), 839–848.
Li, C., Huang, C., Constable, R., Sinha, R., 2006. Imaging response inhibition in a stop-signal task: neural correlates independent of signal monitoring and post-response processing. J. Neurosci. 26 (1), 186–192.
Li, C., Huang, C., Yan, P., Paliwal, P., Constable, R.T., Sinha, R., 2008. Neural correlates of post-error slowing during a stop signal task: a functional magnetic resonance imaging study. J. Cogn. Neurosci. 20 (6), 1021–1029.
Li, C., Morgan, P.T., Matuskey, D., Abdelghany, O., Luo, X., Chang, J.L., Rounsaville, B.J., Y-s, Ding, Malison, R.T., 2010. Biological markers of the effects of intravenous methylphenidate on improving inhibitory control in cocaine-dependent patients. Proc. Natl. Acad. Sci. 107 (32), 14455–14459.
Lim, S., O'Doherty, J., Rangel, A., 2011. The decision value computations in the vmPFC and striatum use a relative value code that is guided by visual attention. J. Neurosci. 31 (37), 13214–13223.
Logan, G., Cowan, W., 1984. On the ability to inhibit thought and action: a theory of an act of control. Psychol. Rev. 91 (3), 295–327.
Logan, G., Schachar, R., Tannock, R., 1997. Impulsivity and inhibitory control. Psychol. Sci. 8 (1), 60–64.
Lu, L.H., Dapretto, M., O'Hare, E.D., Kan, E., McCourt, S.T., Thompson, P.M., Toga, A.W., Bookheimer, S.Y., Sowell, E.R., 2009. Relationships between brain activation and brain structure in normally developing children. Cereb. Cortex 19 (11), 2595–2604.
Lucci, C.R., 2013. Time, Self, and intertemporal choice. Front. Neurosci. 7, 1–5.
Luhmann, C., Chun, M., Yi, D., Lee, D., Wang, X., 2008. Neural dissociation of delay and uncertainty in intertemporal choice. J. Neurosci. 28 (53), 14459–14466.
Luo, S., Ainslie, G., Giragosian, L., Monterosso, J., 2009. Behavioral and neural evidence of incentive bias for immediate rewards relative to preference-matched delayed rewards. J. Neurosci. 29 (47), 14820–14827.
Luo, X., Zhang, S., Hu, S., Bednarski, S.R., Erdman, E., Farr, O.M., Hong, K.-I., Sinha, R., Mazure, C.M., Chiang-shan, R.L., 2013. Error processing and gender-shared and -specific neural predictors of relapse in cocaine dependence. Brain 136 (4), 1231–1244.
Madsen, K., Baaré, W., Vestergaard, M., Skimminge, A., Ejersbo, L., Ramsøy, T., Gerlach, C., Åkeson, P., Paulson, O., Jernigan, T., 2010. Response inhibition is associated with white matter microstructure in children. Neuropsychologia 48 (4), 854–862.
Magen, E., Kim, B., Dweck, C., Gross, J., McClure, S., 2014. Behavioral and neural correlates of increased self-control in the absence of increased willpower. Proc. Natl. Acad. Sci. 111 (27), 9786–9791.
McClure, S., Ericson, K., Laibson, D., Loewenstein, G., Cohen, J., 2007. Time discounting for primary rewards. J. Neurosci. 27 (21), 5796–5804.
McClure, S., Laibson, D., Loewenstein, G., Cohen, J., 2004. Separate neural systems value immediate and delayed monetary rewards. Science 306 (5695), 503–507.
McNamee, D., Rangel, A., O'Doherty, J., 2013. Category-dependent and category-independent goal-value codes in human ventromedial prefrontal cortex. Nat. Neurosci. 16 (4), 479–485.
Metcalfe, J., Mischel, W., 1999. A hot/cool-system analysis of delay of gratification: dynamics of willpower. Psychol. Rev. 106 (1), 3–19.
Moeller, F., Barratt, E., Dougherty, D., Schmitz, J., Swann, A., 2001. Psychiatric aspects of impulsivity. Am. J. Psychiatr. 158 (11), 1783–1793.
Mullette-Gillman, O., Huettel, S., 2009. Neural substrates of contingency learning and executive control: dissociating physical, valuative, and behavioral changes. Front. Hum. Neurosci. 3 (23), 3–19.
Neubert, F., Mars, R., Buch, E., Olivier, E., Rushworth, M., 2010. Cortical and subcortical interactions during action reprogramming and their related white matter pathways. Proc. Natl. Acad. Sci. 107 (30), 13240–13245.
Paloyelis, Y., Asherson, P., Mehta, M.A., Faraone, S.V., Kuntsi, J., 2010. DAT1 and COMT effects on delay discounting and trait impulsivity in male adolescents with attention deficit/hyperactivity disorder and healthy controls. Neuropsychopharmacology 35 (12), 2414–2426.
Peper, J., Mandl, R., Braams, B., de Water, E., Heijboer, A., Koolschijn, P., Crone, E., 2013. Delay discounting and frontostriatal fiber tracts: a combined DTI and MTR study on impulsive choices in healthy young adults. Cereb. Cortex 23 (7), 1695–1702.
Peters, J., Büchel, C., 2010. Episodic future thinking reduces reward delay discounting through an enhancement of prefrontal–mediotemporal interactions. Neuron 66 (1), 138–148.
Peters, J., Büechel, C., 2011. The neural mechanisms of inter-temporal decision-making: understanding variability. Trends Cogn. Sci. 15 (5), 227–239.

Plassmann, H., O'Doherty, J., Rangel, A., 2007. Orbitofrontal cortex encodes willingness to pay in everyday economic transactions. J. Neurosci. 27 (37), 9984–9988.
Poldrack, R., Mumford, J., Schonberg, T., Kalar, D., Barman, B., Yarkoni, T., 2012. Discovering relations between mind, brain, and mental disorders using topic mapping. PLoS Comput. Biol. 8 (10), e1002707.
Ramnani, N., Owen, A., 2004. Anterior prefrontal cortex: insights into function from anatomy and neuroimaging. Nat. Rev. Neurosci. 5 (3), 184–194.
Reiss, A.L., Abrams, M.T., Singer, H.S., Ross, J.L., Denckla, M.B., 1996. Brain development, gender and IQ in children. Brain 119 (5), 1763–1774.
Robbins, T., 2002. The 5-choice serial reaction time task: behavioural pharmacology and functional neurochemistry. Psychopharmacology 163 (3), 362–380.
Schacter, D., Addis, D., Buckner, R., 2007. Remembering the past to imagine the future: the prospective brain. Nat. Rev. Neurosci. 8 (9), 657–661.
Seger, A.C., 2008. How do the basal ganglia contribute to categorization? Their roles in generalization, response selection, and learning via feedback. Neurosci. Biobehav. Rev. 32 (2), 265–278.
Sharp, D., Bonnelle, V., De Boissezon, X., Beckmann, C., James, S., Patel, M., Mehta, M., 2010. Distinct frontal systems for response inhibition, attentional capture, and error processing. Proc. Natl. Acad. Sci. 107 (13), 6106–6111.
Shaw, P., Greenstein, D., Lerch, J., Clasen, L., Lenroot, R., Gogtay, N., Evans, A., Rapoport, J., et al., 2006. Intellectual ability and cortical development in children and adolescents. Nature 440 (7084), 676–679.
Shen, I., Lee, D., Chen, C., 2014. The role of trait impulsivity in response inhibition: event-related potentials in a stop-signal task. Int. J. Psychophysiol. 91 (2), 80–87.
Shin, D., Jung, W., He, Y., Wang, J., Shim, G., Byun, M., Jang, J., Kim, S., Lee, T., Park, H., 2014. The effects of pharmacological treatment on functional brain connectome in obsessive–compulsive disorder. Biol. Psychiatry 75 (8), 606–614.
Solanto, M., Abikoff, H., Sonuga-Barke, E., Schachar, R., Logan, G., Wigal, T., Hechtman, L., Hinshaw, S., Turkel, E., 2001. The ecological validity of delay aversion and response inhibition as measures of impulsivity in AD/HD: a supplement to the NIMH multimodal treatment study of AD/HD. J. Abnorm. Child Psychol. 29 (3), 215–228.
Sowell, E.R., Thompson, P.M., Holmes, C.J., Batth, R., Jernigan, T.L., Toga, A.W., 1999. Localizing age-related changes in brain structure between childhood and adolescence using statistical parametric mapping. NeuroImage 9 (6), 587–597.
Sripada, C., Gonzalez, R., Luan Phan, K., Liberzon, I., 2011. The neural correlates of intertemporal decision-making: contributions of subjective value, stimulus type, and trait impulsivity. Hum. Brain Mapp. 32 (10), 1637–1648.
Swann, A.C., Bjork, J.M., Moeller, F.G., Dougherty, D.M., 2002. Two models of impulsivity: relationship to personality traits and psychopathology. Biol. Psychiatry 51 (12), 988–994.
Swann, N., Cai, W., Conner, C., Pieters, T., Claffey, M., George, J., Aron, A., Tandon, N., 2012. Roles for the pre-supplementary motor area and the right inferior frontal gyrus in stopping action: electrophysiological responses and functional and structural connectivity. NeuroImage 59 (3), 2860–2870.
Tabibnia, G., Monterosso, J., Baicy, K., Aron, A., Poldrack, R., Chakrapani, S., Lee, B., London, E., 2011. Different forms of self-control share a neurocognitive substrate. J. Neurosci. 31 (13), 4805–4810.
van den Bos, W., Rodriguez, C., Schweitzer, J., McClure, S., 2014. Connectivity strength of dissociable striatal tracts predict individual differences in temporal discounting. J. Neurosci. 34 (31), 10298–10310.
van den Bos, W., Rodriguez, C.A., Schweitzer, J.B., McClure, S.M., 2015. Adolescent impatience decreases with increased frontostriatal connectivity. Proc. Natl. Acad. Sci. 112 (29), E3765–E3774.
van Gaal, S., Scholte, H., Lamme, V., Fahrenfort, J., Ridderinkhof, K., 2011. Pre-SMA gray-matter density predicts individual differences in action selection in the face of conscious and unconscious response conflict. J. Cogn. Neurosci. 23 (2), 382–390.
Venkatraman, V., Rosati, A., Taren, A., Huettel, S., 2009. Resolving response, decision, and strategic control: evidence for a functional topography in dorsomedial prefrontal cortex. J. Neurosci. 29 (42), 13158–13164.
Verbruggen, F., Logan, G., 2008. Response inhibition in the stop-signal paradigm. Trends Cogn. Sci. 12 (11), 418–424.
Verbruggen, F., Aron, A., Stevens, M., Chambers, C., 2010. Theta burst stimulation dissociates attention and action updating in human inferior frontal cortex. Proc. Natl. Acad. Sci. 107 (31), 13966–13971.
Vul, E., Harris, C., Winkielman, P., Pashler, H., 2009. Puzzlingly high correlations in fMRI studies of emotion, personality, and social cognition. Perspect. Psychol. Sci. 4 (3), 274–290.
Wang, Q., Luo, S., Monterosso, J., Zhang, J., Fang, X., Dong, Q., Xue, G., 2014. Distributed value representation in the medial prefrontal cortex during intertemporal choices. J. Neurosci. 34 (22), 7522–7530.
White, C., Congdon, E., Mumford, J., Karlsgodt, K., Sabb, F., Freimer, N., London, E., Cannon, T., Bilder, R., Poldrack, R., 2014. Decomposing decision components in the stop-signal task: a model-based approach to individual differences in inhibitory control. J. Cogn. Neurosci. 26 (8), 1601–1614.
Wilbertz, T., Deserno, L., Horstmann, A., Neumann, J., Villringer, A., Heinze, H., Boehler, C., Schlagenhauf, F., 2014. Response inhibition and its relation to multidimensional impulsivity. NeuroImage 103, 241–248.
Xue, G., Aron, A., Poldrack, R., 2008. Common neural substrates for inhibition of spoken and manual responses. Cereb. Cortex 18 (8), 1923–1932.
Xue, G., He, Q., Lu, Z., Levin, I., Dong, Q., Bechara, A., 2013. Agency modulates the lateral and medial prefrontal cortex responses in belief-based decision making. PLoS One 8 (6), e65274.
Yan, C.G., Cheung, B.M., Kelly, C., Colcombe, S.J., Craddock, R.C., Di Martino, A., Li, Q., Zuo, X.N., Castellanos, F.X., Milham, M., 2013. A comprehensive assessment of regional variation in the impact of head micromovements on functional connectomics. NeuroImage 76 (183–201).
Yu, R., 2012. Regional white matter volumes correlate with delay discounting. PLoS One 7 (2), e32595.
Zelazo, P., Carlson, S., 2012. Hot and cool executive function in childhood and adolescence: development and plasticity. Child Dev. Perspect. 6 (4), 354–360.
Zhang, S., Li, CsR, 2012. Functional networks for cognitive control in a stop signal task: independent component analysis. Hum. Brain Mapp. 33 (1), 89–104.